Journal of Materials Chemistry B

Accepted Manuscript

This is an *Accepted Manuscript*, which has been through the Royal Society of Chemistry peer review process and has been accepted for publication.

Accepted Manuscripts are published online shortly after acceptance, before technical editing, formatting and proof reading. Using this free service, authors can make their results available to the community, in citable form, before we publish the edited article. We will replace this *Accepted Manuscript* with the edited and formatted *Advance Article* as soon as it is available.

You can find more information about *Accepted Manuscripts* in the Information for Authors.

Please note that technical editing may introduce minor changes to the text and/or graphics, which may alter content. The journal's standard Terms & Conditions and the Ethical guidelines still apply. In no event shall the Royal Society of Chemistry be held responsible for any errors or omissions in this *Accepted Manuscript* or any consequences arising from the use of any information it contains.

ROYAL SOCIETY OF CHEMISTRY

www.rsc.org/materialsB

A biosensor in nano-size containing valine amino acid organo-modified Cloisite as a bionanohybrid film for immobilization of DNA was developed.

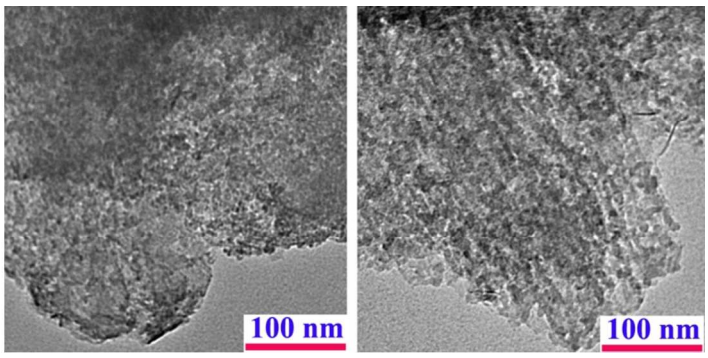

Journal of Materials Chemistry B Accepted Manuscript

Improved immobilization of DNA to graphite surfaces, using amino acid modified clays

Ali A. Ensafi*, Esmaeil Heydari-Bafrooei, Mohammad Dinari, S. Mallakpour

Department of Chemistry, Isfahan University of Technology, Isfahan 84156–83111, Iran

Abstract

Assessment of interaction of small molecules with DNA, hybridization assays for DNA sequence analysis and diagnostics and investigation of DNA damage involve the immobilization of an array of oligonucleotides to a solid substrate. Herein, a new DNA based biosensor in nano size containing valine (Val) amino acid organo-modified Cloisite Na^+ as a new bionanohybrid film for immobilization of DNA was developed. The organoclay of Cloisite–Val was synthesized by a cation-exchange method, which is a displacement of the sodium cations of Cloisite Na^+ with the ammonium ions of the Val-amino acid. The synthesized materials were characterized with different methods such as FT–IR spectroscopy, TEM, SEM, XRD and electrochemical impedance spectroscopy (EIS). Nanostructure film were deposited at the surface of working graphite electrode and utilized for the surface modification with double-stranded DNA. It was found that the electrode modification with DNA and Cloisite-Val leads to an enhanced sensitivity of the DNA voltammetric detection, compared with other modified electrode that used for this work. Efficiencies of DNA immobilization was followed by means of EIS and voltammetry. Immobilization is much more rapid using Cloisite-Val modified graphite supports than employing conventional supports. Stability of the immobilized DNA within several days has been found to be much

Corresponding author: Fax: +98–311–3912350; Tel.: +98–311–3913269; E–mail: Ensafi@cc.iut.ac.ir

Journal of Materials Chemistry B Accepted Manuscript

higher using the new support than in preparations using the conventional ones.

Keywords: DNA immobilization; Graphite surfaces; Amino acid–modified clays.

1. Introduction

In the last two decades, intense research efforts have been paid to DNA biosensors. DNA diagnostics have become an important area of molecular biology and biotechnology studies.[1–3] The detection of specific base sequences in human, viral and bacterial nucleic acids is becoming increasingly important in several areas, with applications ranging from the detection of disease causing and food-contaminating organisms to forensic and environmental research and the monitoring DNA-small molecule interactions.[4–7]

Like other biosensors, DNA sensors are usually in the form of electrodes, chips, and crystals; hence, interaction or hybridization on a sensory surface is a solid-phase reaction. Various techniques, including electrochemical methods, are currently employed for direct confirmation of hybridization or interaction.[8,9] Detection systems are being upgraded to produce more sensitive methods at faster rates.[10] Carbon surfaces are very good materials for electrochemical studies, such as biosensor applications, due to their special allotropes (graphite, diamond and fullerenes/nanotubes).[11] The often-cited advantages of carbon electrodes include low cost, wide potential window, relatively inert electrochemistry, and electrocatalytic activity for a variety of redox reactions.[12,13]

In order to prepare devices based on DNA, the first critical issue to face is related to the immobilization procedures on the surface of the transducer.[14] In view of the impressive advance in the applicability of DNA biosensors, it is important to further enhance the

Journal of Materials Chemistry B Accepted Manuscript

sensitivity of the system; this can be achieved by increasing the amount of immobilized DNA per unit array area. The development of DNA immobilization methodologies that strongly stabilize the DNA on the electrode surface is one key factor in DNA biosensor design.[15] The sensor material and the degree of surface coverage, which directly influences the sensor response is also a critical issue in the development of a DNA electrochemical biosensor for rapid detection of DNA interaction and damage by hazardous compounds.

DNA can be immobilized on sensor surfaces with methods similar to those used for enzyme-based biosensors: adsorption,[16,17] covalent immobilization,[18–20] and avidin (or streptavidin)-biotin interaction.[21,22] These immobilization techniques also can be used to develop DNA microarrays.[23] Immobilization based on adsorption has been reported based on ionic interactions occurring between the negatively charged groups present on the DNA probe and positive charges covering the surface. Non-covalent forces affix the nucleic acid to such materials as nitrocellulose, nylon membranes, or polystryene or metal oxide surfaces such as palladium or aluminum oxide.[24,25] The positive charge can be obtained by means of covering of surface by cationic polycations [26,27] or molecular monolayer functionalized by terminal amine groups.[28] Immobilization based on covalent attachment includes chemisorptions and attachment of DNA on functionalized surfaces.

Immobilizing DNA by means of clay minerals, have attracted the attention of electrochemists. Clay minerals have many desirable properties as electrode surface modifiers: small particle size, large surface area-to-mass ratio, ion-exchange capacity, good intercalation, high stability, flexible adsorption capability and excellent felting property. In green chemistry terms, environmentally friendly analytical protocols and devices, negligible waste, and

Journal of Materials Chemistry B Accepted Manuscript

nontoxic materials make clay minerals of considerable interest to the analytical community.[29,30]

Herein, we report for the first time the use of a nonohybrid of clay and natural amino acid as a substrate for both covalent and electrostatic immobilization of DNA oligonucleotides. We chose Cloisite Na^+ as a kind of montmorillonite (MMT) clay and amino acid valine (Val) as a natural amino acid for preparation of organoclay of Cloisite–Val. The current research focuses on the DNA immobilization on the Cloisite–Val modified electrode and provides a suitable platform for the DNA biosensor fabrication.

2. Experimental section

2.1. Materials

Sodium containing natural MMT was used with the trade name Cloisite Na^+ and cation exchange capacity (CEC) = 92.6 meq/100 g obtained from Southern Clay Products Inc., Texas, USA. S–Valine ($C_5H_{11}NO_2$, 117.15 g mol^{-1}, 99%) and hydrochloric acid (HCl) were purchased from Merck Chemical Co. Analyte solutions were prepared from reagent grade chemicals with deionized water. Deoxyribonucleic acid sodium salt of salmon testes (ds-DNA, catalog No. D1626) and poly(diallyldimethylammonium chloride) (PDDA, low molecular weight) were purchased from Sigma (St. Louis, USA) and used as received. All other chemicals were of reagent grade.

2.2. Apparatus

Electrochemical and impedimetric measurements were performed with an Autolab PGSTAT 12, potentiostat/galvanostat in a conventional three-electrode electrochemical cell using pencil

Journal of Materials Chemistry B Accepted Manuscript

graphite (PG, 0.7–mm diameter, Pentel Co., LTD., Japan) as the working electrode, platinum wire as an auxiliary electrode, and an Ag/AgCl reference electrode in 3.0 mol L^{-1} KCl aqueous media. A standard one-compartment three-electrode cell of 10 mL capacity and a renewable pencil graphite electrode (PGE) was used in all experiments as described in Erdem et al.[32] A Noki pencil was used as a holder for the pencil graphite leads. Electrical contact with the lead was obtained by soldering a metallic wire to the metallic part. The pencil was held vertically with 12 mm of the lead being extruded outside (9 mm of which was immersed in the solution). The convective transport was provided by a magnetic stirrer. All electroanalytical measurements were performed at room temperature.

Electrochemical impedance spectroscopy measurements were carried out in the presence of 5.0 mmol L^{-1} $K_3[Fe(CN)_6]/K_4[Fe(CN)_6]$ as a redox probe in 0.1 mol L^{-1} KCl at a polarization potential of 0.20 V in the frequency range of 0.005 to 10^5 Hz and with an amplitude of 10 mV.

A pH meter, Metrohm (Model 827), with a glass electrode (filled with sat. KCl) was used for pH measurements.

2.3. Preparation of organoclay

The organoclay of Cloisite–Val was synthesized by a cation-exchange method, which is a displacement of the sodium cations of Cloisite Na^+ with the ammonium ions of the Val–amino acid according to our previous study.[31] Briefly, two grams of Cloisite Na^+ was dispersed separately in 150 mL of hot deionized water for 6 h at 80°C. The required amount of S–Val was protonated with stoichiometric amount of concentrated HCl in 50 mL of deionized water and heated at 80 °C for 3 h. These two solutions were mixed and the contents

Journal of Materials Chemistry B Accepted Manuscript

were vigorously stirred for 6 h at 60 °C. The mixture was filtered through a Whatmman® filter paper and then washed about five times with deionized water to remove superficially protonated-tyrosine sorbed on the surface.

2.4. Materials characterization

Fourier transform infrared (FT–IR) spectra were recorded on Jasco-680 (Japan) spectrophotometer with 2 cm^{-1} resolution. The KBr pellet technique was applied for monitoring changes in the FT-IR spectra of the samples in the range of 4000-400 cm^{-1}.

The interlayer spacing of the Cloisite Na^+ and the organoclay of Cloisite–Val was measured by an X–ray diffractometer (XRD) (Bruker, D8 Advance, Germany) with Cu Kα radiation (λ = 0.1542 nm) at 45 kV and 100 mA. The diffraction patterns were collected between 2θ of 1.2o and 10o at a scanning rate of 0.05 o/min. Basal spacing were determined from the position of the d(001) reflection. The d-spacing of the organic bio-nanoclays was analyzed by using Bragg's equation ($n\lambda = 2d\sin\theta$).

The morphology of the Cloisite Na^+ and organoclay of Cloisite–Val was examined by scanning electron microscopy (SEM) (XL30, Philips). The powdered sample was dispersed in H_2O, and then the sediment was dried at room temperature before gold coating. Transmission electron microscopy (TEM) images were obtained using a Philips CM 120 microscope with an accelerating voltage of 100 kV.

2.5. Film assembly

The surface of the PGE was pretreated by applying +1.40 V for 60 s in 0.5 mol L^{-1} acetate buffer (pH 4.8). A 5% (w/v) colloidal dispersion of the Cloisite–Val was prepared by stirring

Journal of Materials Chemistry B Accepted Manuscript

the material in toluene. To assemble the Cloisite–Val /DNA layer by layer films, the PGE was alternately immersed into Cloisite–Val solution for 30 min and into the DNA solution (1.0 mg mL^{-1}, in 0.02 mol L^{-1} tris buffers at pH 7.0 containing 0.02 mol L^{-1} NaCl and 1.0 mmol L^{-1} EDTA) for 10 min with intermediate water washing and nitrogen stream drying. The bare Cloisite–Val–modified PGEs were prepared by following the procedure above without any DNA incorporation into the clay matrix. The prepared Cloisite–Val/DNA films were overoxidized by performing DPV measurements between +0.50 V and +1.40 V at 50 mV pulse amplitude and 10 mV step potential until a steady state response obtained.

2.6. Transduction

A freshly prepared PGE surface was used for each electrochemical measurement. All the experiments were performed at room temperature. All the buffer solutions contained 20 mmol L^{-1} NaCl to establish a constant low ionic strength. The determination of ds-DNA oxidation on the surface of PG, Cloisite–Val /DNA and other modified electrodes was performed with a positive-going differential pulse potential scan (from 0.40 to 1.40), using a pulse amplitude of 50 mV, a modulation time of 0.05 s, and a step potential of 8 mV in the blank solution (0.5 mol L^{-1} acetate buffer (pH 4.8) containing 0.02 mol L^{-1} NaCl. The raw data were treated using the Savitzky and Golay filter (level 2) of the General Purpose Electrochemical Software (GPES) of Eco Chemie (The Netherlands), followed by the GPES software moving average baseline correction, using a “peak width” of 0.01. The procedure was repeated using a new PGE.

3. Results and discussion

Journal of Materials Chemistry B Accepted Manuscript

3.1. Synthesis and characterization

α-Amino acids are one type of the major building blocks of living systems, being the principal components of all naturally occurring peptides and proteins. The use of these compounds in the hybrid materials increases the biocompatibility of such system and allows interactions with biological organism, which are advantageous for bioresorable sutures, screws or plates, tissue engineering scaffolds and drug delivery systems.[32–34] If amino acids were used as a modifier for organo-modification of clays it can be expected to be compatible with a protein/biopeptide matrix. When compared with chemically synthesized modifier, amino acid biosurfactants have the important advantage of biodegradability, low toxicity and various possible structures.[32–34] In this study Cloisite–Val organoclay was prepared via a simple and environmentally friendly ion-exchange method in aqueous solution. Our interest in applying amino acid as a swelling agent stems from the fact that amine group of amino acid can provide cation ($–NH_3^+$) which can form an ionic bond with the negatively charged silicate layers of MMT as well as electrostatic interaction and covalent bond with DNA chains for construction of DNA based biosensor.

3.1. FT–IR Spectroscopy

In the FT–IR spectrum of Cloisite Na^+, the absorption bands at about 3100–3700 cm^{-1} are owing to the O–H stretching and stretching band of hydrogen-bonded water. A weak broad peak at 1639 cm^{-1} is related to H–O–H bending region. The characteristic peaks at 1115 cm^{-1} and 1042 cm^{-1} were due to the out-of-plane Si–O stretching and in-plane Si–O stretching for layered silicates, respectively. Other characteristic vibration peaks at 524 and 468 cm^{-1} are for bending vibration of Si–O and Al–O, respectively (Fig. 1). For organoclay, the absorption

Journal of Materials Chemistry B Accepted Manuscript

peaks were observed with origins being from amino acid molecules. For example, the shoulder FTIR peaks in the range of 2500–3700 cm^{-1} is related to OH stretching of the –COOH group (Fig. 1). The peak at 2960 is attributed to C–H stretching vibration aliphatic hydrocarbon and around 1700 $cm^{-1,}$ it is related to the carbonyl group of the amino acid.

Fig. 1

3.2. X–ray diffraction

The most common technique used to analyze the clay materials is XRD, which measures the interlayer *d*-spacing. The XRD patterns of the Cloisite Na^+ and Cloisite–Val are shown in Fig. 2. Pristine Cloisite Na^+ has an XRD peak at $2\theta = 7.56°$ that was caused by the diffraction of the (001) crystal surface of layered silicates, equaling a *d*-spacing of 1.17 nm. In the XRD pattern of Cloisite–Val, the *d*-spacing of organoclay was 1.49 nm based on Bragg's Law. An increase of the interlayer distance, leads to a shift of the reflection toward lower angles and confirmed that intercalation and surface modification of Cloisite Na^+ had taken place. This means that the basic structures of the Cloisite Na^+ is kept, the layers only propped open, and the basal spacing increased appreciably, provided evidence that intercalation has occurred.

Fig. 2

3.3. SEM and TEM study

SEM is used to investigate the morphology of Cloisite Na^+ and organo-modified clay. The SEM image of Cloisite Na^+ before and after modification with Val is reported in our previous study.[31,] According to the results of the obtained data, there are not many morphologic differences between organoclay despite the obvious variation observed in XRD measurements. The Cloisite Na^+ shows a massive, aggregated morphology and in some

Journal of Materials Chemistry B Accepted Manuscript

instances, there are some bulky flakes. The morphology of the modified clay with Val had more fragments of smaller size formed with irregular shapes.

TEM allows the direct examination of microstructural features resulting from the transformation of clays to organoclays. It has been reported that the layer-structure images of untreated Cloisite Na^+ cannot be observed with TEM.[35,36] It was supposed that for unmodified clay, there is water adsorbed on exchangeable cations such as Na^+. So, the high vacuum of TEM and the high-energy beam can remove the water that makes the layer structures collapse and forbids the structures from being readily observed. Contrasting with unmodified Cloisite Na^+, clay modified with Val–amino acid show layer structures, and the *d*(001) basal spacing are around 12 to 15 Å (Fig. 3). This is almost, in a general agreement with the XRD results.

3.4. Oxidation of the ds-DNA

To evaluate the effect of Cloisite–Val film on the amount of the DNA immobilized on the PG surface, Cloisite–Val–PG electrode was constructed and oxidation voltammograms of guanine and adenine were obtained and compared with other modified electrodes that are often used for immobilization of DNA (MWCNT–PDDA/PG and MWCNT–CHIT/PG). One of the best molecules that are used in immobilization of DNA on the carbon surfaces are carbon nanotubes (CNTs). CNTs are widely used in the fabrication of immunosensors because of their high electrical conductivity, high chemical stability, and extremely high mechanical strength. DNA is an important biological polymer, which is classified as a natural and negatively charged polyelectrolyte due to its phosphate groups. It can be immobilized onto carbon nanotubes via covalent and noncovalent interactions.[37] However, the results are not good enough because negatively charged CNTs repulse the negatively charged DNA.[38] To

Journal of Materials Chemistry B Accepted Manuscript

overcome this problem, the cationic polyelectrolyte such as, Poly(diallyldimethylammonium chloride) (PDDA), chitosan (CHIT) and polyethylenimine are used as dispersant of CNTs.[39] Positively charged PDDA, CHIT and polyethylenimine coat on the negatively charged surface of the CNTs by electrostatic interaction. The polyelectrolyte molecules can combine considerably well with DNA to form DNA films. The CNTs not only display unique electron transfer properties that induce the conductivity of PDDA and improve electron transfer characteristics, they also increase the amount of PDDA deposited on the electrode.

In order to examine the electrochemistry of ds-DNA at various electrode conditions, several experiments were performed. The conditions for the immobilization and oxidation experiments of ds-DNA on the surface of PG, MWCNT–PDDA/PG and MWCNT–CHIT/PG electrodes were discussed elsewhere.[4,5] First of all, the experimental parameters affect the sensitivity are optimized and the experimental results are shown in the supplementary materials. The guanine and adenine bases of ds-DNA oxidized on the surface of carbon electrodes at anodic potentials in acidic media.[4] This oxidation process is used in the detection of small molecules that interact with the ds-DNA. Under the conditions of the experiment, the redox behavior of original ds-DNA immobilized PGE exhibited two oxidation processes of guanine (ca. +1.02 V) and adenine (ca. +1.28 V) residues (Fig. 4a). When DNA/MWCNT–PDDA/PG and DNA/MWCNT–CHIT/PG electrodes were used as the working electrode, the oxidation of guanine and adenine bases of ds-DNA were seen at the peak potential values of +0.91 and +1.21 V (vs. Ag/AgCl) in 0.5 mol L^{-1} ABS containing 20.0 mmol L^{-1} NaCl respectively (Figs. 4b and 4c). Approximately a 100 mV shift was observed in the oxidation peak potentials of guanine and adenine bases of ds-DNA, compared with bare PG. For the comparison, DNA/Cloisite–Val modified PG electrode was also prepared and used in the oxidation

Journal of Materials Chemistry B Accepted Manuscript

experiments. The oxidation of ds-DNA was observed on the surface of the DNA/Cloisite–Val/PG electrode at the peak potential values of +0.72 and +0.93 V (vs. Ag/AgCl) in 0.5 mol L^{-1} acetate buffer containing 20.0 mmol L^{-1} NaCl respectively (Fig. 4e). It can be concluded that the Cloisite–Val nanocomposite modified PG shows an electrocatalytic property and cause a potential shift for the oxidation peak potential of guanine and adenine to the more cathodic values. This positive (catalytic) shift is approximately 300 mV. The electron transfer reaction between the Cloisite–Val electrodes and guanine (or adenine) base of ds-DNA is faster than that of the reaction between the other modified electrodes that are often used for immobilization of DNA (bare PG, MWCNT–PDDA/PG and MWCNT–CHIT/PG) and guanine (or adenine) base of ds-DNA. On the other hand, the oxidation peak currents of guanine and adenine bases of ds-DNA on the surface of Cloisite–Val were increased about 32, 4 and 3 times according to bare PG, MWCNT–CHIT/PG and MWCNT–PDDA/PG electrode, respectively. Increase in the guanine moiety response at DNA/Cloisite–Val, comparing to simple bare PG, MWCNT–PDDA/PG and MWCNT–CHIT/PG is of interest for the DNA detection. It is expected that the obvious increase in the detecting signal of guanine (or adenine) base of ds-DNA is due to the participation of certain surface functional groups of amino acid that increase amount of DNA immobilization.

Fig. 4

3.5. Electrochemical characteristics of the DNA marker

$Co(phen)_3^{3+}$ was used as electroactive indicator to detect the DNA molecule using cyclic voltammetry. Table 1 shows the current and potential data of the oxidation differential pulse signal of $Co(phen)_3^{3+}$ obtained at the DNA/Cloisite–Val/PGE, Cloisite–Val modified PG and the other modified electrodes that are often used for immobilization of DNA. Concerning the

Journal of Materials Chemistry B Accepted Manuscript

PGEs covered with nanomodifiers, the peak potential data for the DNA marker show a positive (catalytic) shift at both MWCNT and Cloisite–Val modified electrodes, but, this shift is more pronounced for the electrode modified with the Cloisite–Val. The DNA deposited at the Cloisite–Val layer leads to further increase of the $Co(phen)_3^{3+}$ peak current, compared with other electrodes (Table 1). Hence, the nanostructured Cloisite–Val film used can be covered effectively by ds-DNA. The efficiency of the Cloisite–Val composite coverage could be due to better access of DNA by the marker particles within the nanostructured films of enhanced active surface area. The higher efficiency of DNA/Cloisite–Val/PGE comparing to other modified PGEs is evidently due to participation of certain functional groups of amino acid at adsorption of DNA. Thus, the amperometric response obtained with the DNA/Cloisite–Val/PG electrode proves that modification of electrode with Cloisite–Val allows the increase of DNA immobilization capacity and sensitivity. This offers an attractive prospect for using such films in DNA damage assays and DNA–molecules interactions.

Table 1

Dependences of the peak current of $Co(phen)_3^{3+}$ on accumulation time follow typical adsorption isotherm shape with signal saturation from about 90 s for DNA/Cloisite–Val modified PGE and about 300 s for MWCNT modifiers. On the other hand, the kinetics of accumulation of DNA marker on the Cloisite–Val has a faster isotherm in contrast to MWCNT modified PGEs. In accordance with data in Table 1, the modification of the bare PGE electrodes with simple nanostructured film of MWCNT and Cloisite–Val leads to the increase of the $Co(phen)_3^{3+}$ signal due to its adsorption (on MWCNT and Cloisite–Val) or electrostatic chemisorption (on Cloisite–Val).

Journal of Materials Chemistry B Accepted Manuscript

3.6. Electrochemical impedance spectroscopy

Previous studies have revealed that the amount of assembly of nucleic acids on the support can be followed by electrochemical impedance spectroscopy, EIS [26]. Figure 5 show a Nyquist plot of impedance for PGE electrodes with different modifiers. In the Nyquist plot of impedance spectra, the semicircle portion at higher frequencies corresponds to the electron-transfer-limited process and the linear portion seen at lower frequencies may be ascribed to the diffusion. The increase in the diameter of the semicircle reflects the increase in the interfacial charge-transfer resistance (Rct). In general, the modification of the PG electrode with nanomodifiers causes a decrease in the surface impedance and, on the other hand, DNA enhances the impedance. As shown in Fig. 5A, effect of the DNA nanomodifier composite is different. The Rct of the bare PG electrode was 5200 Ω; the value decreased to 2800 and 3700 Ω with the deposition of PDDA–MWCNT and Cloisite–Val, respectively. After immobilization of ds-DNA on the PDDA–MWCNT and Cloisite–Val, the value of Rct increased to 5000 and 10000 Ω, respectively. The increase in Rct is due to the immobilization of negatively charged ds-DNA on the electrode surface resulting in a negatively charged interface that electrostatically repels the negatively charged redox probe $[Fe(CN)_6]^{3-/4-}$ and inhibits interfacial charge-transfer [26]. As shown in Fig. 5, increase in Rct after immobilization of DNA on the Cloisite–Val modified PGE was greater, compared with MWCNT. EIS data shows that the nanostructured Cloisite–Val film has a superior ability for immobilization of DNA on the surfaces. This feature represents a novelty at the electrochemical detection of ds-DNA damage.

Fig. 5

3.7. Effect of ionic strength

Journal of Materials Chemistry B Accepted Manuscript

It is well known that the interactions are impacted by the ionic strength of the solution when the binding mode of molecules with DNA is electrostatic mode. At low ionic strength values the electrostatic interaction mode between a molecule and the negative phosphate backbone of DNA is predominant, and conversely, at high ionic strength values the negative charges of DNA phosphates are shielded, consequently, electrostatic interaction decreased. Thus the effect of the ionic strength on the interaction of nanostructured Cloisite–Val film with DNA was addressed by DPV in the NaCl concentration range from 0 to 100 mM. For this purpose, the Cloisite–Val /DNA layer by layer films was assembled using alternately immersion of PGE into Cloisite–Val solution for 30 min and into the DNA solution (1.0 mg mL^{-1}, in 0.02 mol L^{-1} tris buffers at pH 7.0 containing different concentration of NaCl and 1.0 mmol L^{-1} EDTA) for 10 min with intermediate water washing and nitrogen stream drying. In Fig. 6, the experiments performed at both, low (20.0 mM NaCl) and high (100.0 mM NaCl) ionic strength are shown. As shown in Fig. 6, the current of guanine oxidation decreased by increasing the NaCl concentration. This fact suggests that DNA can interact electrostatically with Cloisite–Val film and when the charges of phosphate groups present in DNA are shielded, the interaction decreases and amount of immobilized DNA diminishes.

3.8. Stability of the biosensor

The DNA marker signal measurement repeated within several days at the same biosensor was used to test the sensor stability. Between the measurements, the sensors were stored under dry conditions at open air and room temperature. The working stability is characterized by a RSD value of the marker peak current obtained from 4 consecutive measurements where the RSD values are 9% and 10% for DNA/MWCNT–PDDA/PG and DNA/MWCNT–CHIT/PG

Journal of Materials Chemistry B Accepted Manuscript

electrodes, respectively. The total stability was tested during the 19 days period by measuring the marker signal every 3rd day. The RSD values reached to 19% (n = 10) for DNA/MWCNT–PDDA/PG and 27% (n=10) for DNA/MWCNT–CHIT/PG electrode. In case of DNA/Cloisite–Val/PG modified electrode, the working and total stability is characterized by RSD of 4% (n = 4) and 5% (n = 6), respectively. This improved stability can satisfy voltammetric assay of the interactions of the surface attached ds-DNA, compared with other electrodes. It was not possible to use the electrodes for more than one measurement and they, therefore, had to be replaced each time.

4. Conclusions

In the work discussed in this report, amino acid valine modified clay has been devised for effective immobilization of DNA on the graphite electrodes. Cloisite–Val modified electrodes have shown to be an interesting support for DNA immobilization. The existence of amino groups in amino acid structures can dramatically improve immobilization rates by covalent immobilization. Moreover, the storage stability of the immobilized DNA was better than those of conventional supports. Therefore, this support can be recommended as a new tool for DNA immobilization in DNA hybridization, damage and interaction assays.

Acknowledgement

The authors wish to thank the Research Council of Isfahan University of Technology (IUT), the Center of Excellence in Sensor and Green Chemistry, and the Iranian Nanotechnology Initiative Council for their support.

Journal of Materials Chemistry B Accepted Manuscript

References

1 D. P. Little, T. J. Cornish, M. J. O'Donnell, A. Braun, R. J. Cotter and H. Köster, *Anal. Chem.*, 1997, **69**, 4540.

2 P. B. Monaghan, K. M. McCarney, A. Ricketts, R. E. Littleford, F. Docherty, W. E. Smith, D. Graham J. M. Cooper, *Anal. Chem.*, 2007, **79**, 2844.

3 E. Donatin and M. Drancourt, *Med. Maladies Infect.*, 2012, **42**, 453.

4 A. A. Ensafi, M. Amini, B. Rezaei, *Sens. Actuators B*, 2013, **177**, 862.

5 A. A. Ensafi, E. Heydari-Bafrooei, B. Rezaei, *Biosens. Bioelectron.*, 2013, **41**, 627.

6 A. Dey, A. Kaushik, S. K. Arya and S. Bhansali, *J. Mater. Chem.*, 2012, **22**, 14763.

7 A. A. Ensafi, E. Heydari-bafrooei and M. Amini, *Biosens. Bioelectron.*, 2012, **31**, 376.

8 K. R. Meier and M. Gratzel, *Chem. Phys. Chem.*, 2002, **3**, 371.

9 F. Patolsky, A. Lichtenstein and I. Willner, *J. Am. Chem. Soc.* 2001, **123**, 5194.

10 R. M. Kong, Z. L. Song, H. M. Meng, X. B. Zhang, G. L. Shen and R. Q. Yu, 2014, **54**, 442.

11 R. L. McCreery, *Chem. Rev.*, 2008, **108**, 2646.

12 A. Walcarius, *Trends Anal. Chem.*, 2012, **38**, 79.

13 Z. Peng, D. Zhang, L. Shi and T. Yan, *J. Mater. Chem.*, 2012, **22**, 6603.

14 M. I. Pividori, A. Merkoc and S. Alegret, *Biosens. Bioelectron.*, 2000, **15**, 291.

15 A. M. O. Brett, in *Bioelectrochemistry: Fundamentals, Experimental Techniques and Applications* ed. Bartlett, P., John Wiley & Sons, Ltd., 2008, Ch. 12, pp. 416.

16 C. M. A. Brett, A. M. O. Brett and S. H. P. Serrano, *J. Electroanal. Chem.*, 1994, **366**, 225.

17 M. L. Pedano and G. A. Rivas, *Electrochem. Commun.*, 2004, **6**, 10.

18 X. Jianga and X. Lin, *Analyst*, 2005, **130**, 391.

Journal of Materials Chemistry B Accepted Manuscript

19 B. P. Corgier, A. Laurent, P. Perriat, L. J. Blum and C. A. Marquette, *Angew Chem. Int. Ed. Engl.*, 2007, **46**, 4108.

20 A. Ruffien, M. Dequaire and P. Brossier., *Chem Commun*, 2003, **7**, 912.

21 R. M. Iost and F. N. Crespilho, *Biosens. Bioelectron.*, 2012, **31**, 1.

22 D. J. Chung, K. C. Kim and S. H. Choi, *Appl. Surf. Sci.*, 2011, **257**, 9390.

23 N. Zammatteo, L. Jeanmart, S. Hamels, S. Courtois, P. Louette, L. Hevesi and J. Remacle, *Anal. Biochem.*, 2000, **280**, 143.

24 J. R. Fernandes, D. H. Grant and M. Ozsoz, *Anal. Chem.*, 1997, **69**, 4056.

25 J. Wang, X. Cai, G. Rivas, H. Shiraishi and N. Dontha, *Biosens. Bioelectron.*, 1997, **12**, 587.

26 A. A. Ensafi, E. Heydari-Bafrooei and B. Rezaei, *Anal. Chem.*, 2013, **85**, 991.

27 A. A. Ensafi, M. Amini and B. Rezaei, *Biosens. Bioelectron.*, 2014, **53**, 43.

28 C. Douarche, R. Cortès, C. H. Villeneuve, S. J. Roser and A. Braslau, *J. Chem. Phys.*, 2008, **128**, 1.

29 C. Mousty, *Appl. Clay Sci.* 2004, **27**, 159.

30 J. Zima, J. Barek and J. Labuda, *Electroanalysis* 2006, **18**, 163.

31 S. Mallakpour and M. Dinari, *Appl. Clay Sci.*, 2011, **51**, 353.

32 A. Gigante, C. Chillemi, C. Bevilacqua, F. Greco, F. Bisaccia and A. M. Tamburro, *J. Mater. Sci. Mater. Med.*, 2003, **14**, 717.

33 M. A. Pilkington-Miksa, M. J. Writer, S. Sarkar, Q. H. Meng, S. E. Barker, P. A. Shamlou, H. C. Hailes, S. L. Hart and A. B. Tabor, *Bioconjugate Chem.*, 2007, **18**, 1800.

34 G. Tosi, L. Costantino, F. Rivasi, B. Ruozi., E. Leo., A. V. Vergoni, R. Tacchi, A. Bertolini, M. A. Vandelli and F. Forni, *J. Controlled Release*, 2007, **122**, 1.

Journal of Materials Chemistry B Accepted Manuscript

35 S. Mallakpour and M. Dinari, *J. Therm. Anal. Calorim.*, 2013, **111**, 611.

36 Y. Xi, R. L. Frost, H. He, T. Kloprogge and T. Bostrom, *Langmuir*, 2005, **21**, 8675.

37 P. G. He and M. Bayachou, *Langmuir*, 2005, **21**, 6086.

38 M. J. Gong, T. Han, C. X. Cai, T. H. Lu and J. Y. Du, *J. Electroanal. Chem.*, 2008, **623**, 8.

39 N. Li, H. W. Zhao, R. Yuan, K. F. Peng and Y. Q. Chai, *Electrochim. Acta*, 2008, **54**, 235.

Journal of Materials Chemistry B Accepted Manuscript

Table 1 Peak current and peak potential of the marker $Co(phen)_3^{3+}$ obtained after its 120 s accumulation from 0.10 μmol L^{-1} solution in PBS (pH 7.0) before and after the modification of the corresponding PGE.

Electrode	Ip (μA)	Ep (V)
Bare PGE	0.21±0.05	–0.120
DNA/PGE	2.01±0.21	–0.118
DNA/PDDA–MWCNT/PGE	4.23±0.28	–0.129
DNA/CHIT–MWCNT/PGE	2.94±0.17	–0.127
Cloisite–Val/PGE	2.04±0.23	–0.132
DNA/Cloisite–Val/PGE	12.32±0.52	–0.139

Journal of Materials Chemistry B Accepted Manuscript

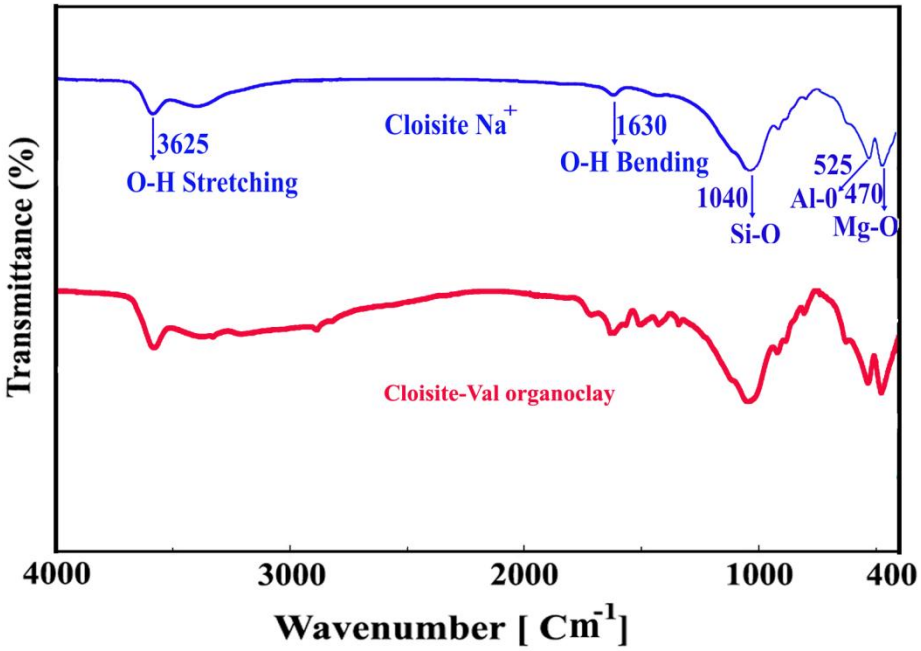

Figure 1 FT–IR (KBr) spectra of Cloisite Na^+ and organo-modified clay.

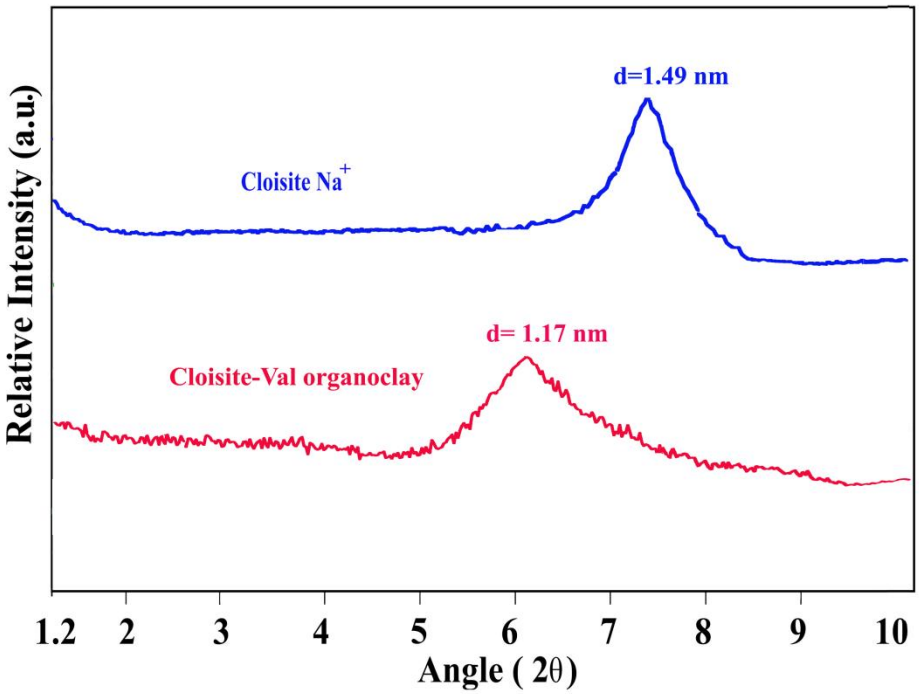

Figure 2 XRD patterns of Cloisite Na^+ and Cloisite–Val.

Journal of Materials Chemistry B Accepted Manuscript

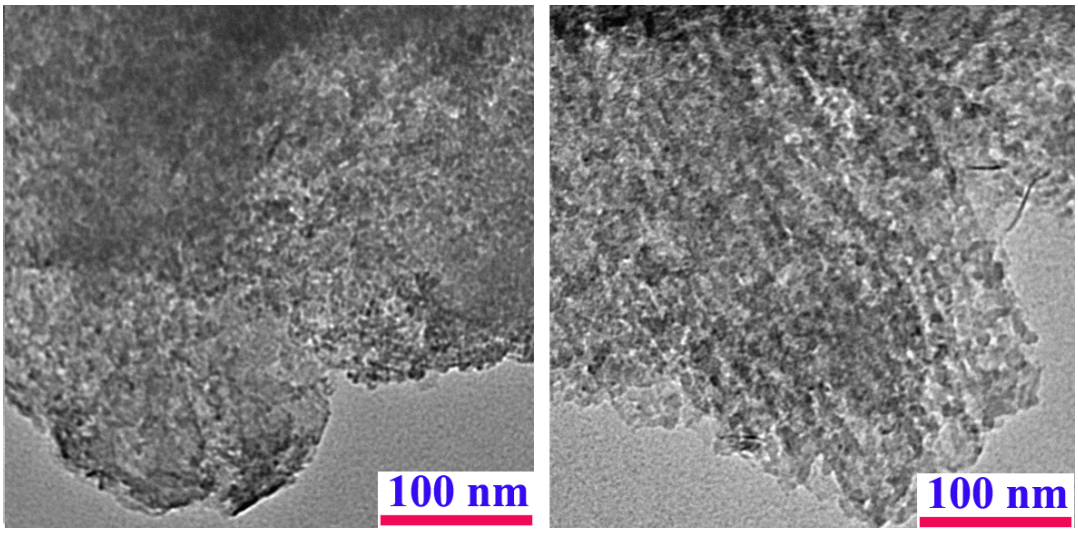

Figure 3 TEM images of the modified clay with Val.

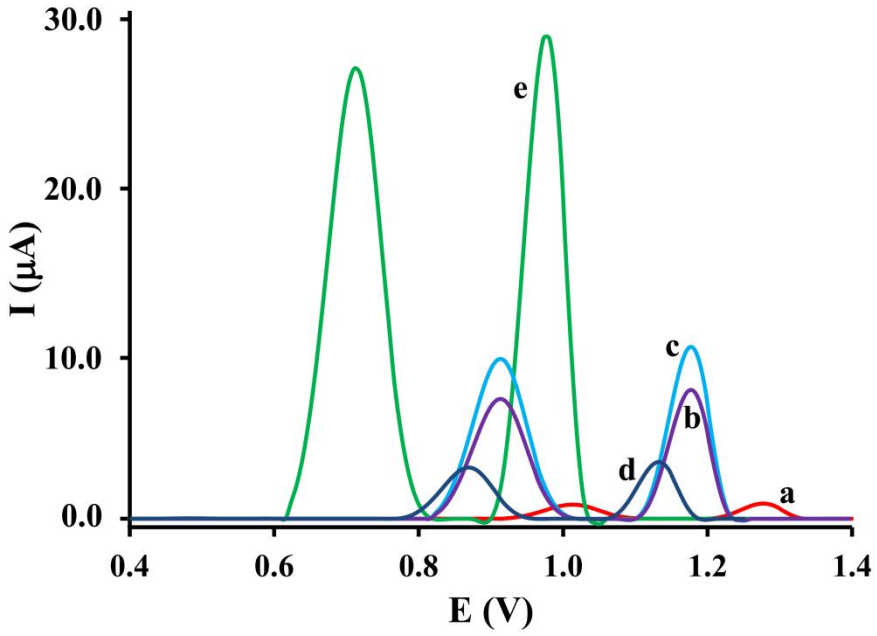

Figure 4 Differential pulse voltammograms of guanine and adenine at the surface of (a) DNA–PGE, (b) DNA/MWCNT–CHIT/PGE, (c) DNA/MWCNT–PDDA/PGE (d) DNA/Cloisite/PGE, and (e) DNA/Cloisite–Val/PGE. Conditions: scanning potential between +0.40 and +1.40 V in acetate buffer (pH 4.8).

Journal of Materials Chemistry B Accepted Manuscript

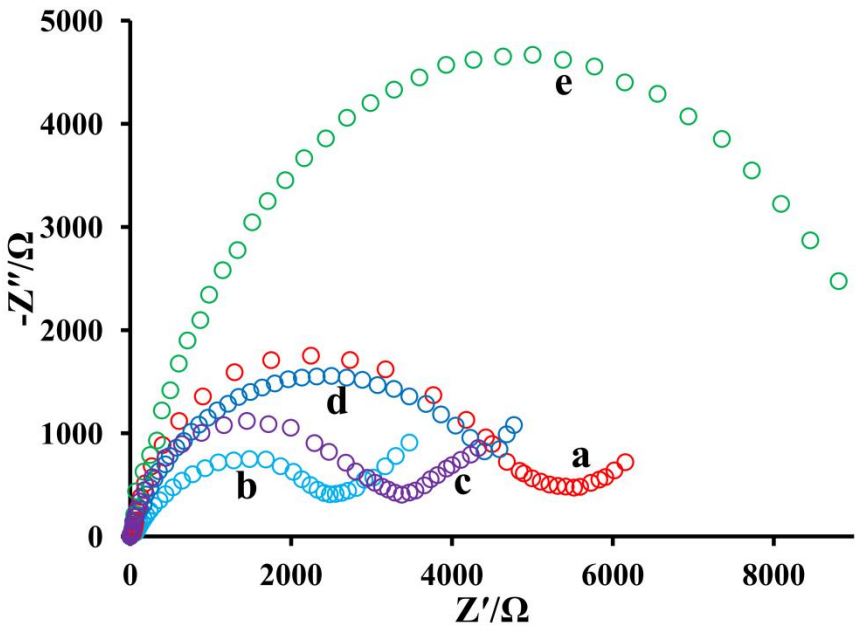

Figure 5 Impedance spectra of (a) bare PGE, (b) MWCNT–PDDA/PGE, (c) Cloisite–Val/PGE, (d) DNA/MWCNT–PDDA/PGE, and (e) DNA/Cloisite–Val/PGE.

Journal of Materials Chemistry B Accepted Manuscript

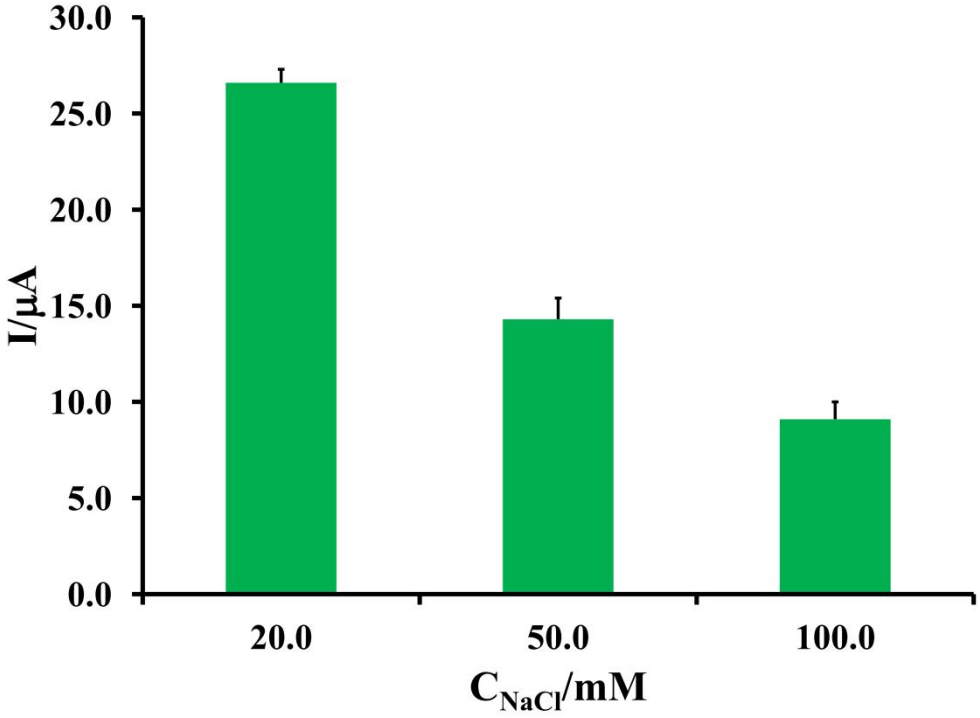

Figure 6 Effect of NaCl concentration on the immobilization of 1.0 μg mL^{-1} DNA on the DNA/Cloisite–Val/PGE. Immobilization time: 10 min.

Journal of Materials Chemistry B Accepted Manuscript